Load Distribution in the Typical and Zero Cells in a PLP-PPP Vehicular Communication Network

Kaushlendra Pandey, Kanaka Raju Perumalla, Abhishek K. Gupta, Harpreet S. Dhillon

Abstract

This paper has modeled a vehicular network where the roads are modeled as Poisson line process (PLP), and vehicles on the roads are modeled as Poisson point process (PPP). We call this point process as Cox process driven by PLP or PLP-PPP. The position of BSs are modeled as 2 dimensional (2D) Poisson point process. First, we derive the PGF for the load (number of vehicular users) distribution on the typical BS and the BS serving a typical vehicle (or tagged BS). Using the PGFs, we derive the loads' mean and variance. Using the load distribution, we have derived the closed form expressions for the rate coverage and meta distribution of the rate coverage. Finally, we derive the CDF of kth contact distance (CD) and nearest neighbor distance (NND) for the PLP-PPP. We have presented two applications where the distance distributions can be used for analyzing the vehicular network. We have performed extensive simulations to test the accuracy of obtained results.

I. Introduction

Vehicular communication involves exchanging traffic data, safety messages, and entertainment services. This exchange of data may happen between a vehicle to established infrastructure network such as cellular BS or between two vehicles. For example, a vehicle may get information about nearby traffic, road conditions, and entertainment services from the nearby base station (BS) that also provides connectivity to static users. This communication is also called a vehicle to infrastructure (V2I) communication. Similarly, a vehicle may get critical information such as the speed of the nearby vehicle, conditions on the road, and accidents by connecting it with

K. Pandey, K. Raju Perumalla and A. K. Gupta are with IIT Kanpur, India, 208016. Email:{kpandey,pkraju,gkrabhi}@iitk.ac.in. H. S. Dhillon is with Wireless@VT, Bradley Department of Electrical and Computer Engineering, Virginia Tech, Blacksburg, VA 24061 (Email: hdhillon@vt.edu).

its nearest vehicles this communication is termed as a vehicle-to-vehicle (V2V) communication. Implementing vehicular communication (V2V and V2I) provides a safe and seamless flow of traffic on the road which consequences as frequent change of serving BS for moving vehicle. Another example is in a city with a crowded road network, the vehicular users put an extra load (number of vehicles served by BS) on a cellular base station. It becomes challenging for BS to allocate the BW to newly admitted vehicular users in the cell. The burden of additional load due to the vehicle may be reduced by enabling data sharing and content broadcasting in V2V communication. However, to enable such communication, a vehicle has to know the distances of its nearby vehicles. Inspired by these two problems in V2I (*i.e.* load on infrastructure network) and V2V (*i.e.* SNR distribution during the broadcast of a vehicle) network, we perform a load distribution, that is the number of vehicles served by a BS and rate coverage that is the data rate obtained by a vehicle from a BS, analysis of V2I network. Furthermore, for a V2V network, we perform a signal-to-noise ratio (SNR) analysis from a vehicle to its nearest kth vehicle. For the purpose of analysis we model the vehicles, roads and BSs using the well accepted tools of stochastic geometry (SG) [1], [2].

Literature survey The SG has been widely used for the modeling and analysis of vehicular networks. A commonly used method for analyzing vehicular networks is by modeling the random orientation of lines using Poisson line process (PLP), and random location of vehicles on each road as Poisson point process. Such a point process is known as the Poisson Cox process driven by Poisson line process or PLP-PPP [1], [2]. In [3] authors presented a detailed approach for modeling, analysis various extensions for the system level analysis of vehicular networks using PLP-PPP. For more details and examples on the modeling of vehicular networks as PLP-PPP and the cellular BSs as PPP readers are requested to refer to [3]–[5] and reference therein. However we present few work that are closely related to V2I vehicular network. For example, in [5]–[8] authors derive the downlink coverage probability for a typical receiver with a different transmitter association scheme. For load distribution and rate coverage analysis in [9] authors derived the PMF for the load distribution for a randomly selected BS (or typical BS) and BS serving a typical vehicle (or tagged BS). Furthermore, using the load distribution authors derived the rate coverage for vehicular user. The method adopted by the authors are specific for PLP-PPP and can not extended for other point processes which can be used for modeling and analysis of vehicular network. Apart from that in vehicular network individual link reliability from a BS is an important metric to establish a seamless data traffic in V2I network. The meta distribution of

rate coverage is metric that measures the individual link's rate coverage for a given realization. In this paper present a generalized method for deriving the load distribution and also derive the meta distribution for rate coverage.

A V2V communication involves the communication between the two vehicles. In [10], [11] author performed the vehicular network analysis for V2V network. In these works, some of the vehicles acts as transmitter and some of them acts as receiver. Then based on the nearest transmitter association authors derived the coverage probability. In such works authors need the probability distribution of contact distance (CD) and nearest neighbor distance (NND), which is derived in [4], [10], [11] using different methods such as LF or PGFL of PLP-PPP. A moving vehicle broadcasts some time critical information such as its velocity, time when it is going to apply break continuously to its nearby vehicles. For a broadcasting vehicle, it becomes important to fix the signal power in such a way that it can establish a communication link to its kth nearest vehicle. Such form of analysis have not been reported in the literature so far. In this paper we attempt to analyze the SNR distribution for a broadcasting vehicle to its nearest kth vehicle. Inspired by the problems mentioned above in this paper we perform a load distribution and SNR distribution analysis for a vehicular network. The important contribution of this paper is as follows.

Contribution

1) This paper presents the PGF for the load distribution on a typical and tagged BS in a vehicular network. Using the properties of PGFs, we derive the mean and variance of the load.
2) This paper presents a simpler expressions for the rate coverage expression for a vehicle. To test the individual link's rate coverage for given realization we present the meta distribution of the rate coverage.
3) For V2V networks, this paper performs a SNR distribution analysis from a broadcasting vehicle to its nearest kth vehicle. In the process of deriving the SNR distribution we present the kth CD and NND distribution for PLP-PPP, which have its own applications in the analysis of vehicular networks.
4) Finally, the method adopted in deriving the load distribution for PLP-PPP is generalized in nature and can be adopted for any point process super imposed on the line of PLP for example PLP-TCP *i.e.* point on the PLP have distribution according the Thomas cluster process [12].

Now, we present the important notations that we are going to use throughout the paper.

Notation A vector in $\mathbb{R}^2$ and $\mathbb{R}$ is denoted by bold style letter ($\mathbf{x}$) and bold *italic* style ($\boldsymbol{x}$) with their norms $||\mathbf{x}||$ and $|\boldsymbol{x}|$ respectively. One dimension (1-D) and two dimensional (2-D) ball centered at $\boldsymbol{x}$ and $\mathbf{x}$ of radius r is denoted by $\mathbf{b}_1(\boldsymbol{x}, r)$ and $\mathbf{b}_2(\mathbf{x}, r)$ respectively. For a set A, $|\mathsf{A}|$ denotes the Lebesgue measure of set A, for example $|\mathbf{b}_1(\mathrm{o}, r)| = 2r$. For a point process Ψ, the notation $\Psi(\mathsf{B})$ denotes number of points of Ψ falling inside the set B. The PGF, CDF and PDF of any random X variable is denoted by $\mathcal{P}_X(\cdot)$, $F_X(\cdot)$ and $f_X(\cdot)$ respectively. The expected value and variance of random variable X is denoted by $\mathbb{E}[X]$ and $\mathrm{Var}[X]$ respectively. For a RV X with PGF $\mathcal{P}_X(s)$ the mean and the variance of the RV X is

$$\mathrm{Var}[X] = [\mathcal{P}_X^{(2)}(s)]_{s=1} + \mathbb{E}[X] - (\mathbb{E}[X])^2 \tag{1}$$

$$\mathbb{E}[X] = \left[\mathcal{P}_X^{(1)}(s)\right]_{s=1}, \tag{2}$$

The Gamma distribution of a random variable X is

$$g_X(a_1, b_1, c_1, x) = a_1 b_1^{c_1/a_1} (\Gamma(c_1/a_1))^{-1} x^{c_1-1} e^{-b_1 x^{a_1}}. \tag{3}$$

The Faà di Bruno's formula [13], which states that the k-th derivative $\frac{\mathrm{d}^k}{\mathrm{d}s^k} \exp(h(s))$ of $\exp(h(s))$ with respect to s is given as

$$= \exp(h(s)) \sum_{\mathrm{N}_k} \frac{k!}{n_1! \cdots n_k!} \left(h^{(1)}(s)/1!\right)^{n_1} \cdots \left(h^{(k)}(s)/k!\right)^{n_k}, \tag{4}$$

where the sum is over set N_k consisting of all $k-$tuples $\{n_1 \cdots n_k\}$ with $n_i \geq 0$ and $n_1 + 2n_2 + \ldots + kn_k = k$.

II. System Model

The network of roads are modeled as the lines of Poisson line process (PLP) $\Phi_{\boldsymbol{l}} = \{\boldsymbol{l}_1, \boldsymbol{l}_2, \ldots\}$ with density $\lambda_{\boldsymbol{l}}$. In a PLP of density $\lambda_{\boldsymbol{l}}$, the average number of lines hitting a convex body $\mathcal{K}$ with perimeter $L(\mathcal{K})$ is $\lambda_{\boldsymbol{l}} L(\mathcal{K})$. A ith line $\boldsymbol{l}_i \in \Phi_{\boldsymbol{l}}$ is uniquely characterized by the two parameters ρ_i and ϕ_i in the representation space $\mathbf{C}^* \equiv \mathbb{R} \times [0,\, \pi]$. Here, ρ_i is the length of the normal from origin to line $\boldsymbol{l}_i$, and ϕ_i is the angle between the normal and positive x-axis. The ith line of $\Phi_{\boldsymbol{l}}$ located in the representation space ($\mathbf{C}^*$) at (ρ_i, ϕ_i) is uniquely characterized by $(\rho_i \cos\phi_i, \rho_i \sin\phi_i) \in \mathbb{R}^2$. The location $(\rho_i \cos\phi_i, \rho_i \sin\phi_i) \in \mathbb{R}^2$ is the point on the line which is nearest to the origin.

Vehicle's location on road: We model the location of vehicular users on each road as 1-D PPP. Let $\Psi = \{\psi_1, \psi_2, \ldots\}$ be independent and identically distributed PPP on each road of $\Phi_{\boldsymbol{l}}$ having

density λ. Hence, on the road $\boldsymbol{l}_i$ the position of vehicles is modeled as PPP ψ_i. Therefore the location of jth vehicle of $\boldsymbol{l}_i$ in $\mathbb{R}^2$ is

$$\mathbf{x}_{i,j} = \left(\rho_i \cos\phi_i + \boldsymbol{x}_j \sin\phi_i,\ \rho_i \sin\phi_i - \boldsymbol{x}_j \cos\phi_i\right),$$

where $\boldsymbol{x}_j$ denotes the location of jth vehicle in ψ_i on the line $\boldsymbol{l}_i$ for $\rho_i = 0, \phi_i = 0$. Hence, taking the union of all the points located on each line forms a PLP-PPP as

$$\Psi_{\mathrm{p}} = \bigcup_{\boldsymbol{l}_i \in \Phi_{\boldsymbol{l}}} \bigcup_{\psi_i \in \Psi} \psi_i,\ \forall\{i,j\} \in \mathbb{N} = \mathbf{x}_{i,j}.$$

where $\mathbf{x}_{i,j} \in \mathbb{R}^2$ denotes the jth point of ψ_i on the line $\boldsymbol{l}_i$. The density λ_{p} of Ψ_{p} is $\pi\lambda_{\boldsymbol{l}}\lambda$ [4].

BS's location: We model the BS's location as 2D PPP $\Phi_b \equiv \{\mathbf{y}_i\}$ with density λ_b. Further the association of a vehicle from its serving BS is average power association based technique. Therefore the serving region of a typical BS is its associated Voronoi region. To be prcise the Voronoi region of a typical BS at $\mathbf{y}$, $V_{\mathbf{y}}$ is defined as

$$V_{\mathbf{y}} = \{\mathbf{x} \in \mathbb{R}^2 : \mathbf{y} = \arg\min_{\mathbf{y}_i \in \Phi_b} \|\mathbf{x} - \mathbf{y}_i\|\}.$$

Before starting the main technical section of this paper, we present few essential probability distributions related to Poisson Voronoi cell of a typical BS. We frequently use these distributions throughout the paper.

Area, perimeter and chord length distribution of a typical BS Let the Voronoi region associated with a typical BS is denoted by V_{t} with area $|V_{\mathrm{t}}|$ and perimeter Z. Therefore, the PDF of $|V_{\mathrm{t}}|$ and Z are [14]

$$f_{|V_{\mathrm{t}}|=v_{\mathrm{t}}}\left(|v_{\mathrm{t}}|\right) = \lambda_b g\left(1.07950, 3.03226, 3.31122, \lambda_b v_{\mathrm{t}}\right), \tag{5}$$

$$f_{Z=z}(z) = \sqrt{\lambda_b}/4 g\left(2.33609, 2.97006, 7.58060, \sqrt{\lambda_b} z/4\right), \tag{6}$$

where $g(\cdot)$ denotes the generalized Gamma distribution define in (3). The length distribution $f_C(c)$ of typical chord [15] is

$$f_{C=c}(c) = (\pi/2)\lambda_b^{\frac{3}{2}} \int_0^{\pi}\int_0^{\infty} \left[\lambda_b \left(\mathcal{V}^{(1)}(c,y,r(c,\theta))\right)^2 - \mathcal{V}^{(2)}(c,y,r(c,\theta))\right] e^{-\lambda_b \mathcal{V}(c,y,r(c,\theta))} y \mathrm{d}y \mathrm{d}\theta. \tag{7}$$

where $\mathcal{V}(c,y,r(c,\theta))$ is the union of two disk of radius y and $r(c,\theta)$ with centers c distance away, $\mathcal{V}^{(k)}(\cdot)$ denotes the kth derivative of $\mathcal{V}(\cdot)$ with respect ot c and $r(c,\theta) = \sqrt{y^2 + c^2 - 2yc\cos\theta}$. In a serving region of a typical BS, the length of the road in the serving region will be the chord of typical Voronoi cell. The maximum length of a chord in Voronoi cell is going to play a

critical role in the analysis of load distribution. Hence we present important properties related to the maximum length of chord and dependency of chord over the parameter of a typical Voronoi cell.

Proposition 1. *For a convex polygon with given perimeter the maximum length of the chord is upper bounded by half of the perimeter. (For proof see Appendix A)*

Proposition 2. *The length of chords of a typical Voronoi cell conditioned on the perimeter are dependent variable. The length distribution of a typical chord conditioned on the perimeter $Z = z$ is (for proof see Appendix B)*

$$f_C^{'}(c) = \frac{f_C(c)\mathbb{1}(0 \leq c \leq z/2)}{F_C(z/2)}. \tag{8}$$

Since we have presented the important results related to probability distribution of area, perimeter and chord length its dependency on perimeter therefore, we can start the main technical section of this paper.

III. Analysis of vehicular network

In this section first we present the load distribution on a typical and the tagged BS.

Load distribution on typical BS The load on a typical BS is defined as the number of vehicular users falling in the serving region of a BS. Therefore, mathematically we say that the load on a typical BS is number of points of Φ_{p} falling a typical Voronoi cell of Φ_b. We present two methods of approximating the load named Approximation-1 (Approx-1) and Approximation-2 (Approx.-2) to on a typical BS. Let the load on a typical BS is denoted by S_{p} and its approximation corresponding to Approx.-1 and Approx.-2 is denoted by $\widehat{S}_{\mathrm{p}}$ and $\widetilde{S}_{\mathrm{p}}$ respectively. Now, we briefly present the method adopted to find the $\widehat{S}_{\mathrm{p}}$ and $\widetilde{S}_{\mathrm{p}}$.

Approx.-1: The approximation-1 is based on the method presented in [9] where authors first derive the Laplace functional (LF) of sum W of chord lengths in a typical Voronoi cell of given perimeter Z. To derive the LF, authors assumed that chords lengths of typical Voronoi cell with given perimeter are independent random variables. Then authors used the PGFL of PLP and deconditioned with the perimeter distribution Z. Further, after obtaining the LF of sum W of chords and using the facts that a number of points of PLP-PPP falling in W is Poisson distributed with mean λW, authors derived the PMF of load as a derivative of LF. In this paper, conditioned Z and assuming that the chords of a typical Voronoi with a given perimeter are independent

(which is the inaccurate assumption for the details see the proof of Proposition 2), we find the PGF of load. Here we would like to underline that finding PGF provides miscellaneous insights of a random variable such as mean, variance, skewness or pth moment. Such statistical properties are helpful to visualize the distribution of load for an extensive range of parameters such as BS density or vehicular density etc.

Approx.-2: Approx.-2 is obtained by approximating the area of a typical Voronoi cell with a circle of radius R_{t}. Similar to Approximation-1 in this approach in [9] authors first derive the LF of the sum of chords and then using the property of PPP authors derived the PMF of $\widetilde{S}_{\mathrm{p}}$. However in this paper we derive the PGF of $\widetilde{S}_{\mathrm{p}}$. The approach we adopted is flexible and can be used for other Cox processes driven by Poisson line process. In this paper conditioned on the length of a single chord we derive the PGF for the number of points falling on that chord which is Poisson distributed. Now using the PGFL of PLP we derive the PGF of $\widetilde{S}_{\mathrm{p}}$. This approach can also be adopted for the cluster process (such as Thomas cluster process) on each line of PLP which can not be obtained using the methods presented in [9].

Theorem 1. *(Approximation-1) The PGF $\mathcal{P}_{\widehat{S}_{\mathrm{p}}}(s)$ for the load on the typical Voronoi is (For proof see Appendix C)*

$$= \int_{z=0}^{\infty} \exp\left(-\lambda_{\boldsymbol{l}} z \left(1 - \int_0^{z/2} \exp\left(\lambda c(s-1)\right) f_C^{'}(c)\mathrm{d}c\right)\right) f_{Z=z}(z)\mathrm{d}z. \tag{9}$$

The PMF of S_{p} is

$$\mathbb{P}\left[S_{\mathrm{p}} = k\right] = \int_0^{\infty} \exp\left(h_{\mathrm{p}}(0,z)\right) \sum_{\mathsf{N}_k} \frac{\left(h_{\mathrm{p},1}(z)\right)^{n_1} \cdots \left(h_{\mathrm{p},k}(z)\right)^{n_k}}{n_1! \cdots n_k!} f_{Z=z}(z)\mathrm{d}z, \tag{10}$$

where $h_{\mathrm{p}}(s,z)$ and $h_{\mathrm{p},k}(z)$ is,

$$h_{\mathrm{p}}(s,z) = \lambda_{\boldsymbol{l}} z \left(\int_0^{z/2} e^{\lambda c(s-1)} f_C^{'}(c)\mathrm{d}c - 1\right),\ h_{\mathrm{p},k}(z) = \left(\lambda_{\boldsymbol{l}} z/k!\right) \int_0^{z/2} \left(\lambda c\right)^k e^{-\lambda c} f_C^{'}(c)\mathrm{d}c. \tag{11}$$

The load on the typical Voronoi cell can be approximated to a load $\widetilde{S}_{\mathrm{p}}$ on circle of area equal to the area of typical Voronoi cell $|V_{\mathrm{t}}|$. Let radius of circle be $R_{\mathrm{t}} = \sqrt{|V_{\mathrm{t}}|/\pi}$ hence distribution of R_{t}, $f_{R_{\mathrm{t}}} = 2\pi r_{\mathrm{t}} f_{|V_{\mathrm{t}}|}(\pi r_{\mathrm{t}}^2)$ ($f_{|V_{\mathrm{t}}|}(\cdot)$ is given in (5)).

Theorem 2. *(Approximation-2) The PGF $\mathcal{P}_{\widetilde{S}_{\mathrm{p}}}(s)$ of load on the typical cell V_{t} in Ψ_{p} is (for proof see Appendix D.)*

$$\mathcal{P}_{\widetilde{S}_{\mathrm{p}}}(s) = \int_{r_{\mathrm{t}}=0}^{\infty} \exp\left(-2\pi\lambda_{\boldsymbol{l}} \left(r_{\mathrm{t}} - \int_0^{r_{\mathrm{t}}} \frac{\exp\left(2\lambda(s-1)t\right)t\mathrm{d}t}{\sqrt{r_{\mathrm{t}}^2 - t^2}}\right)\right) f_{R_{\mathrm{t}}}(r_{\mathrm{t}})\mathrm{d}r_{\mathrm{t}}. \tag{12}$$

The PMF of $\widetilde{S}_{\rm p}$ is

$$\mathbb{P}\left[\widetilde{S}_{\rm p}=k\right]=\int_0^{\infty}\exp\left(-2\pi\boldsymbol{\lambda_l}r_{\rm t}+g_{{\rm p},0}(r_{\rm t})\right)\sum_{\mathsf{N}_k}\frac{(g_{{\rm p},1}(r_{\rm t}))^{n_1}\cdots(g_{{\rm p},k}(r_{\rm t}))^{n_k}}{n_1!\cdots n_k!}f_{R_{\rm t}}(r_{\rm t})\mathrm{d}r_{\rm t}, \quad (13)$$

where,

$$g_{{\rm p},k}(r_{\rm t})=2\pi\boldsymbol{\lambda_l}(2\lambda)^k\int_0^{r_{\rm t}}\frac{t^{k+1}e^{-2\lambda t}}{\sqrt{r_{\rm t}^2-t^2}}\mathrm{d}t. \quad (14)$$

Using the properties of PGF presented in (1), now we derive the mean and the variance of the two approximation.

Corollary 2.1. *The mean and the variance of $\widetilde{S}_{\rm p}$ and $\widehat{S}_{\rm p}$ is (for proof see Appendix E)*

$$\mathbb{E}\left[\widetilde{S}_{\rm p}\right]=\lambda_{\rm p}\pi\mathbb{E}\left[R_{\rm t}^2\right]\overset{(a)}{=}\lambda_{\rm p}/\lambda_b,\ \mathbb{E}\left[\hat{S}_{\rm p}\right]=\frac{\lambda_{\rm p}}{\pi}\mathbb{E}[Z]\mathbb{E}[C]\overset{(b)}{=}\lambda_{\rm p}/\lambda_b, \quad (15)$$

where (a) is obtained because $\mathbb{E}[R_{\rm t}^2]=1/(\pi\lambda_b)$ and (b) is achieved as $\mathbb{E}[C]=\pi/(4\sqrt{\lambda_b})$ [15], $\mathbb{E}[Z]=4/\sqrt{\lambda_b}$.

$$\mathrm{Var}[\widetilde{S}_{\rm p}]=(\pi\lambda_{\rm p})^2\mathbb{E}[r_{\rm t}^4]+(16/3)\,\lambda\lambda_{\rm p}\mathbb{E}[r_{\rm t}^3]+\lambda_{\rm p}/\lambda_b-(\lambda_{\rm p}/\lambda_b)^2\,. \quad (16)$$

$$\mathrm{Var}[\widehat{S}_{\rm p}]=(\lambda_{\rm p}/\pi)^2\,\mathbb{E}[Z^2]\,(\mathbb{E}[C])^2+(\lambda_{\rm p}/\pi)\lambda\mathbb{E}[C^2]\mathbb{E}[Z]+\mathbb{E}[\widehat{S}_{\rm p}]-\left(\mathbb{E}[\widehat{S}_{\rm p}]\right)^2. \quad (17)$$

Load on the tagged BS: A tagged BS serves the typical vehicle of $\Psi_{\rm p}$. Let the typical vehicles is located at the origin therefore the BS's cell serving the typical vehicle is the tagged cell. Let the tagged cell is denoted by $V_{\rm t_o}$. Precisely we can define the tagged cell as

$$V_{\rm t_o}=\{\mathbf{x}\in\mathbb{R}^2:\arg\min_{\mathbf{y}_i\in\Phi_b}\|\mathbf{x}-\mathbf{y}_i\|\leq\arg\min_{\mathbf{y}_i\in\Phi_b}\|\mathbf{y}_i\|\}.$$

As the perimeter distribution of tagged cell is not available in the literature we can not find the approximate load on tagged cell using the method presented in the Approximation-1. However, using the Approximation-2, we can approximate the load on the tagged cell by considering it as a circle $\mathbf{b}_2(\mathbf{y},R_{\rm o})$ of radius $R_{\rm o}$ centered at the the BS $\mathbf{y}$ serving the typical vehicle located at the origin. The area of equal to the tagged Voronoi cell. Hence, $R_{\rm o}=\sqrt{|V_{\rm t_o}|/\pi}$ then the distribution of $R_{\rm o}$ is

$$f_{R_{\rm o}}(r_{\rm o})=2\pi^2\lambda_b r_{\rm o}^3 f_{|V_{\rm t}|}(r_{\rm o}). \quad (18)$$

Further the length of the tagged chord passing through the typical vehicle can be obtained using the length bias sampling [9] which is given as

$$f_{C_{\rm o}}(c_{\rm o})=\frac{c_{\rm o}f_C(c_{\rm o})}{\mathbb{E}[C]}=\frac{4\sqrt{\lambda_b}}{\pi}c_{\rm o}f_C(c_{\rm o}). \quad (19)$$

Load on tagged BS PLP-PPP: Now, we derive the load distribution on the tagged base station for $\Psi_{\rm p}$. Let $\widetilde{M}_{\rm p}$ denotes the approximate load on the tagged cell.

Theorem 3. *The PGF $\mathcal{P}_{\widetilde{M}_{\rm p}}(s)$ and PMF of the the load $\widetilde{M}_{\rm p}$ on the tagged BS in $\Psi_{\rm p}$ is (for proof see Appendix F)*

$$= \int_{c_{\rm o}=0}^{\infty}\int_{r_{\rm o}=0}^{\infty} e^{\lambda c_{\rm o}(s-1)} \exp\left(-2\pi\lambda_{\boldsymbol{l}}\left(r_{\rm o} - \int_0^{r_{\rm o}} \frac{e^{2\lambda(s-1)t}t{\rm d}t}{\sqrt{r_{\rm o}^2-t^2}}\right)\right) f_{R_{\rm o}}(r_{\rm o}){\rm d}r_{\rm o} f_{C_{\rm o}}(c_{\rm o}){\rm d}c_{\rm o}. \quad (20)$$

The PDF of $R_{\rm o}$ and $C_{\rm o}$ is given is (18) *and 19 respectively. The PMF $\mathbb{P}\left[\widetilde{M}_{\rm p}=m+1\right]$ is:*

$$= \sum_{k=0}^{m}\binom{m}{k}\int_{r_{\rm o}=0}^{\infty}\exp\left(-2\pi\lambda_{\boldsymbol{l}}r_{\rm o}+g_{{\rm p},0}(r_{\rm o})\right)\sum_{\mathsf{N}_k}\frac{(g_{{\rm p},1}(r_{\rm o}))^{n_1}\cdots(g_{{\rm p},k}(r_{\rm o}))^{n_k}}{n_1!\cdots n_k!}f_{R_{\rm o}}(r_{\rm o}){\rm d}r_{\rm o}$$
$$\times\int_{c_{\rm o}=0}^{\infty}(\lambda c_{\rm o})^{m-k}\exp\left(-\lambda c_{\rm o}\right)f_{C_{\rm o}}(c_{\rm o}){\rm d}c_{\rm o},$$

where $g_{{\rm p},k}(\cdot)$ is provided in (14).

Corollary 3.1. *The mean load on the tagged BS with $\mathbb{E}\left[r_{\rm o}^2\right]=\frac{1.28}{\pi\lambda_b}$ is*

$$\mathbb{E}\left[\widetilde{M}_{\rm p}\right]=\lambda_{\rm p}\pi\mathbb{E}[R_{\rm o}^2]+\lambda_{\rm p}\mathbb{E}[C_{\rm o}]=\frac{1.28\lambda_{\rm p}}{\lambda_b}+\frac{4\sqrt{\lambda_b}\lambda_{\rm p}}{\pi}\mathbb{E}[C^2].$$

Similarly, we can derive the variance of $\widetilde{M}_{\rm p}$. The second derivative $\mathcal{P}^{(2)}_{\widetilde{M}_{\rm p}}(s)$ of the PGF at $s=1$ is

$$\left[\mathcal{P}^{(2)}_{\widetilde{M}_{\rm p}}(s)\right]_{s=1}=(\pi\lambda_{\rm p})^2\mathbb{E}\left[R_{\rm o}^4\right]+\frac{16}{3}\lambda\lambda_{\rm p}\mathbb{E}[R_{\rm o}^3]+\frac{2.48\lambda\lambda_{\rm p}}{\lambda_b}\mathbb{E}[C_{\rm o}]+\lambda^2\mathbb{E}[C_{\rm o}^2], \quad (21)$$

using the second derivative and (1) *we get the variance of $\widetilde{M}_{\rm p}$.*

Using the load distributions, now we derive the rate coverage and meta distribution for the rate coverage.

Rate Coverage The rate coverage is defined as the probability that the average rate achieved by the typical receiver is greater than a certain threshold. To derive rate coverage without loss of generality, we assume that the typical vehicular user is located at the origin. Let all the BSs transmit the equal unit power, and the typical receiver (located at origin) connects with the nearest base station. Furthermore, we have assumed that the BS with zero load is not transmitting power to save the transmission energy. Therefore, the active base station density that contribute to the interference power is ${\rm p_{on}}=\mathbb{P}[\widetilde{S}_{\rm p}=0]$. Hence, the signal to interference ratio is given by

$${\rm SIR}=\frac{h_0R^{-\alpha}}{\sum_{\mathbf{y}\in\Phi_b'}h_{\mathbf{y}}||\mathbf{y}||^{-\alpha}},$$

where $\Phi_b^{'}$ is the active BS PPP with density $\lambda_b \mathrm{p_{on}}$, R denotes the distance of nearest BS, α is the path loss exponent, h_0 and $h_{\mathbf{y}}$ denotes the fading gain of the typical receiver link and the gains of rest of the links respectively. Further we have assumed that the fading coefficients h is exponentially distributed with unit mean. Assuming that the bandwidth B is equally shared by all user associated with a typical serving region, the achievable rate of the typical receiver is given by

$$\mathcal{R} = \left(B/\left(\widetilde{M}_{\mathrm{p}} + 1\right)\right) \log_2 \left(1 + \mathrm{SIR}\right).$$

Hence, the rate coverage for a typical receiver is defined as

$$\mathbf{R}_c(\tau) = \mathbb{P}(\mathcal{R} > \tau).$$

In [16] the coverage probability is provided as

$$\mathbb{P}[\mathrm{SIR} > \tau] = 2\pi\lambda_b \int_0^{\infty} r \exp\left(-\lambda_b \pi r^2 - \mathrm{p_{on}} \int_r^{\infty} \frac{2\pi\lambda_b \tau y \mathrm{d}y}{\tau + (y/r)^{\alpha}}\right) \mathrm{d}r \tag{22}$$

$$\stackrel{(a)}{=} \frac{1}{1 + \mathrm{p_{on}} \int_1^{\infty} \frac{\mathrm{d}t}{1+t^{\alpha/2}\tau^{-1}}}. \tag{23}$$

The step (a) is achieved by substituting $\lambda_b \pi y^2 = u$ and $u = vt$. Using the definition of $\mathbf{R}_c(\tau)$, we get the following

Theorem 4. *The rate coverage for the typical receiver is*

$$\mathbf{R_c}(\theta(\tau)) = \sum_{m=0}^{\infty} \mathbb{P}(\widetilde{M}_{\mathrm{p}} = m) \frac{1}{1 + \mathrm{p_{on}} \int_1^{\infty} \frac{\mathrm{d}t}{1+t^{\alpha/2}\theta^{-1}}} \tag{24}$$

where $\theta(\tau) = 2^{\frac{(m+1)\tau}{B}} - 1$. *Replacing the value of* $\mathbb{P}(\widetilde{M}_{\mathrm{p}} = m)$ *for* Ψ_{p}, *we get rate coverage for a typical vehicular user.*

Meta Distribution for rate Coverage We can find the meta distribution [17] for any individual link dependent performance metrics such as coverage probability, rate coverage. For example the meta distribution of the rate coverage is defined as

$$\overline{F}_{P_{\mathrm{r}}(\tau)}(x) = \mathbb{P}(P_{\mathrm{r}}(\tau) > x), \forall x = [0,\, 1],$$

where $P_{\mathrm{r}}(\tau)$ is the probability that rate coverage is greater than threshold τ conditioned on a realization of point process Ψ_{p} and load on the tagged BS $\widetilde{M}_{\mathrm{p}}$. Precisely, we can write it as

$$P_{\mathrm{r}}(\tau) = \mathbb{P}\left(\mathcal{R} > \tau | \widetilde{M}_{\mathrm{p}}, \Psi_{\mathrm{p}}\right).$$

Further, it is inconvenient to derive the meta distribution directly. Therefore, first we derive the moments of $P_{\mathrm{r}}(\tau)$. Then, using the Gill Pelaez inversion theorem [18], we derive the meta distribution $\overline{F}(t,\tau)$ of rate coverage $\mathbf{R_c}(\tau)$. The relation between the qth moment of $P_{\mathrm{r}}(\tau)$ and the rate coverage $\overline{F}(t,\theta)$ is

$$\mathsf{M}_q(\tau) = \mathbb{E}\left[(P_{\mathrm{r}}(\tau))^q\right] = \int_0^1 q t^{q-1}\overline{F}(t,\tau)\mathrm{d}t, \tag{25}$$

for $q=1$, $\mathsf{M}_1(\tau)$ denotes the coverage probability.

Theorem 5. *The q-th moment of the downlink coverage probability and the rate coverage probability respectively is (for proof see Appendix G)*

$$\mathsf{M}_q(\tau) = \int_{u=0}^{\infty} \exp\left(-2\mathrm{p_{on}}u\int_{z=0}^{1}\left(1-\frac{1}{(1+\tau z^{\alpha})^q}\right)\frac{\mathrm{d}z}{z^3}\right)e^{-u}\mathrm{d}u \tag{26}$$

$$\mathsf{S}_q(\theta(\tau)) = \sum_{m=0}^{\infty}\mathbb{P}(\widetilde{M}_{\mathrm{p}}=m)\mathsf{M}_q\left(\theta(\tau)\right), \tag{27}$$

where $\theta(\tau) = 2^{\frac{(m+1)\tau}{B}} - 1$.

Using the Theorem 5, the definition of meta distribution and Gil-Pelaez lemma inversion theorem [18], we can derive the meta distribution for the rate coverage.

Theorem 6. *The meta distribution for rate coverage is (for proof see Appendix H)*

$$\overline{F}_{P_{\mathrm{r}}(\tau)}(x) = \frac{1}{2} - \frac{1}{\pi}\sum_{m=0}^{\infty}\mathbb{P}(\widetilde{M}_{\mathrm{p}}=m)\int_{t=0}^{\infty}\sin\left(t\ln(x)+\Theta(t,\theta(\tau))\right)\frac{\mathrm{d}t}{t} \tag{28}$$

where

$$\Theta(t,\theta(\tau)) = \tan^{-1}\left(\frac{f_{1,i}(t,\theta(\tau))}{f_{1,r}(t,\theta(\tau))+1}\right),$$

and $f_r(t,\theta(\tau),z) = \cos\left(t\ln\left(1+\theta(\tau)z^{\alpha}\right)\right)$, $f_i(t,\theta(\tau),z) = \sin\left(t\ln\left(1+\theta(\tau)z^{\alpha}\right)\right)$ *and* $f_{1,i}(t,\theta(\tau)) = 2\mathrm{p_{on}}\int_{z=0}^{1}\left(1-f_i(t,\theta(\tau),z)\right)\frac{\mathrm{d}z}{z^3}$ *and* $f_{1,r}(t,\theta(\tau)) = 2\mathrm{p_{on}}\int_{z=0}^{1}\left(1-f_r(t,\theta(\tau),z)\right)\frac{\mathrm{d}z}{z^3}$

A. β approximation model

Another simple yet tractable approach is the β approximation for the meta distribution [17]. For the β approximation [17], [19], we can use first and the second moment of $\mathsf{S}(\theta(\tau))$ to get the meta distribution.

$$\overline{F}_{P_{\mathrm{r}}(\tau)}(x) = 1 - I_x\left(\frac{\mathsf{S}_1(\theta(\tau))\left(\mathsf{S}_1(\theta(\tau))-\mathsf{S}_2(\theta(\tau))\right)}{\mathsf{S}_2(\theta(\tau))-\mathsf{S}_1^2(\theta(\tau))}, \frac{(\mathsf{S}_1(\theta(\tau))-\mathsf{S}_2(\theta(\tau)))(1-\mathsf{S}_1(\theta(\tau)))}{\mathsf{S}_2(\theta(\tau))-\mathsf{S}_1{}^2(\theta(\tau))}\right),$$

where $I_x(\cdot)$ is the regularized incomplete beta function.

$$\mathsf{S}_1(\theta(\tau)) = \sum_{m=0}^{\infty} \mathbb{P}(\widetilde{M}_{\mathrm{p}} = m)\mathsf{M}_1(\theta(\tau)), \mathsf{S}_2(\theta(\tau)) = \sum_{m=0}^{\infty} \mathbb{P}(\widetilde{M}_{\mathrm{p}} = m)\mathsf{M}_2(\theta(\tau))$$

The approach we have presented to derive the Approximation-2 of load may be used to derive the kth CD and NND for the PLP-PPP. The kth CD and NND plays a critical role in the analysis of wireless network [20]. For example, the kth distance distributions are frequently used to determine the coverage probability under the dominant interference.

Distance distributions: Now we present the CDFs and PDFs for the kth CD and NND for PLP-PPP.

kth CD: The kth CD is defined as the distance of the kth point of Ψ_{p} from an arbitrary point in $\mathbb{R}^2$. Let the number $S_{\mathrm{p}}(r)$ denotes the points of Ψ_{p} falling in $\mathbf{b}_2(\mathrm{o}, r)$. From the definition of kth CD as

$$F_{R_k}(r) = 1 - \sum_{m=0}^{k-1} \mathbb{P}\left[S_{\mathrm{p}}(r) = m\right].$$

Hence using Theorem 2 eq. (13), we get the following result.

Theorem 7. *The kth CD for Ψ_{p} is*

$$F_{R_k}(r) = 1 - \sum_{m=0}^{k-1} \exp\left(-2\pi\lambda_{\boldsymbol{l}} r + g_{\mathrm{p},0}(r)\right) \sum_{\mathsf{N}_m} \frac{(g_{\mathrm{p},1}(r))^{n_1} \cdots (g_{\mathrm{p},k}(r))^{n_m}}{n_1! \cdots n_m!}, \tag{29}$$

where $g_{\mathrm{p},k}(r)$ is provided in (14)*.*

Corollary 7.1. *The CDF and PDF of CD for $k = 1, 2$ is*

$$F_{R_1}(r) = 1 - e^{-2\pi\lambda_{\boldsymbol{l}} r + g_{\mathrm{p},0}(r)},\ f_{R_1}(r) = \exp\left(-2\pi\lambda_{\boldsymbol{l}} r + g_{\mathrm{p},0}(r)\right)\left(g^{(1)}_{\mathrm{p},0}(r) - 2\pi\lambda_{\boldsymbol{l}}\right) \tag{30}$$

$$F_{R_2}(r) = 1 - e^{-2\pi\lambda_{\boldsymbol{l}} r + g_{\mathrm{p},0}(r)}\left(1 + g_{\mathrm{p},1}(r)\right), f_{R_2}(r) = f_{R_1}(r)(1 + g_{\mathrm{p},1}(r)) - e^{-2\pi\lambda_{\boldsymbol{l}} r + g_{\mathrm{p},0}(r)} g^{(1)}_{\mathrm{p},1}(r) \tag{31}$$

nth NND: Similar to kth CD, the nth NND is defined as the distance of nth nearest point from the typical point of Ψ_{p}. Without loss of generality, we assume that the typical point is located at the origin hence $\mathrm{o} \in \Psi_{\mathrm{p}}$. Let $M_{\mathrm{p}}(r)$ denote the number of points number of points of $\Psi_{\mathrm{p}} \setminus \{\mathrm{o}\}$ falling in $\mathbf{b}_2(\mathrm{o}, r)$ conditioned on $\mathrm{o} \in \Psi_{\mathrm{p}}$. From the definition [21], CDF of nth NND is

$$F_{R'_n}(r) = 1 - \sum_{m=0}^{n-1} \mathbb{P}\left[M_{\mathrm{p}}(r) = m\right].$$

The CDF of nth NND can be derived using the similar method presented in the proof of Theorem 3.

Theorem 8. *The CDF $F_{R'_n}(r)$ for nth NND of Ψ_{p} is*

$$= 1 - \sum_{m=0}^{n-1} \sum_{k=0}^{m} \binom{m}{k} e^{(-2\pi\lambda_{\boldsymbol{l}} r + g_{\mathrm{p},0}(r))} \sum_{\mathsf{N}_k} \frac{(g_{\mathrm{p},1}(r))^{n_1} \cdots (g_{\mathrm{p},k}(r))^{n_k}}{n_1! \cdots n_k!} \int_{c_{\mathrm{o}}=0}^{\infty} (\lambda c_{\mathrm{o}})^{m-k} e^{-\lambda c_{\mathrm{o}}} f_{C_{\mathrm{o}}}(c_{\mathrm{o}}) \mathrm{d}c_{\mathrm{o}}, \tag{32}$$

where $g_{p,k}$ is provided in (14)*.*

Corollary 8.1. *The CDF and PDF of NND for $n = 1, 2$ is*

$$F_{R'_1}(r) = 1 - \exp\left(-2\pi\lambda_{\boldsymbol{l}} r + g_{\mathrm{p},0}(r)\right) \int_{c_{\mathrm{o}}=0}^{\infty} \exp\left(-\lambda c_{\mathrm{o}}\right) f_{C_{\mathrm{o}}}(c_{\mathrm{o}}) \mathrm{d}c_{\mathrm{o}}, \tag{33}$$

$$f_{R'_1}(r) = \exp\left(-2\pi\lambda_{\boldsymbol{l}} r + g_{\mathrm{p},0}(r)\right) \left(2\pi\lambda_{\boldsymbol{l}} - g^{(1)}_{\mathrm{p},0}(r)\right) \int_{c_{\mathrm{o}}=0}^{\infty} \exp\left(-\lambda c_{\mathrm{o}}\right) f_{C_{\mathrm{o}}}(c_{\mathrm{o}}) \mathrm{d}c_{\mathrm{o}}. \tag{34}$$

$$\begin{aligned} F_{R'_2}(r) = {} & 1 - \exp\left(-2\pi\lambda_{\boldsymbol{l}} r + g_{\mathrm{p},0}(r)\right) \left(1 + g_{\mathrm{p},1}(r)\right) \int_{c_{\mathrm{o}}=0}^{\infty} \exp\left(-\lambda c_{\mathrm{o}}\right) f_{C_{\mathrm{o}}}(c_{\mathrm{o}}) \mathrm{d}c_{\mathrm{o}} \\ & - \exp\left(-2\pi\lambda_{\boldsymbol{l}} r + g_{\mathrm{p},0}(r)\right) \int_{c_{\mathrm{o}}=0}^{\infty} (\lambda c_{\mathrm{o}}) \exp\left(-\lambda c_{\mathrm{o}}\right) f_{C_{\mathrm{o}}}(c_{\mathrm{o}}) \mathrm{d}c_{\mathrm{o}}, \end{aligned} \tag{35}$$

$$\begin{aligned} f_{R'_2}(r) = {} & \left(1 + g_{\mathrm{p},1}(r)\right) f_{R'_1}(r) - \exp\left(-2\pi\lambda_{\boldsymbol{l}} r + g_{\mathrm{p},0}(r)\right) g^{(1)}_{\mathrm{p},1}(r) \int_{c_{\mathrm{o}}=0}^{\infty} \exp\left(-\lambda c_{\mathrm{o}}\right) f_{C_{\mathrm{o}}}(c_{\mathrm{o}}) \mathrm{d}c_{\mathrm{o}} \\ & + \exp\left(-2\pi\lambda_{\boldsymbol{l}} r + g_{\mathrm{p},0}(r)\right) \left(2\pi\lambda_{\boldsymbol{l}} - g^{(1)}_{\mathrm{p},0}(r)\right) \int_{c_{\mathrm{o}}=0}^{\infty} (\lambda c_{\mathrm{o}}) \exp\left(-\lambda c_{\mathrm{o}}\right) f_{C_{\mathrm{o}}}(c_{\mathrm{o}}) \mathrm{d}c_{\mathrm{o}}. \end{aligned} \tag{36}$$

Coverage analysis in non line of sight communication: Turning our interest to applications of distance distribution in vehicular networks. We assume that the BS and the vehicles broadcasts messages to the other vehicles to communicate various data set. For wireless propagation along urban roads, the pathloss model should be different for line- and non-light-of-sight (NLoS) vehicles [22, Fig. 5]. The vehicles with NLoS connections suffer from serious diffraction losses due to the propagation of wireless signals around the corner. In Fig. 5 (a) the distribution of the signal-to-noise ratio (SNR) for the 10 nearest vehicles with LoS connection to the BS depicted. Assuming a distance-based propagation pathloss $r^{-\alpha}$, where r stands for the distance of vehicles from BS, and a diffraction loss L, it is straight- forward to convert the distance distributions into received signal level distributions. Then, it also remains to scale the obtained CDFs by the noise power level N_o. Specifically, for the k-th nearest vehicle with NLoS connection the SNR

from BS to vehicle and vehicle to vehicle is

$$\mathrm{SNR}_{k,\mathrm{b2v}} = \frac{\mathrm{L}R_k^{-\alpha}}{N_o}. \tag{37}$$

Theorem 9. *The SNR distribution for kth LOS vehicle for* $\mathrm{b2v}$ *is*

$$F_{\mathrm{SNR},k}(\tau) = \mathbb{P}[\mathrm{SNR}_k \leq \tau] = \mathbb{P}\left[\frac{\mathrm{L}R_k^{-\alpha}}{N_o} \leq \tau\right] = 1 - \mathbb{P}\left[R_k \leq \left(\frac{\tau N_o}{\mathrm{L}}\right)^{-1/\alpha}\right] \tag{38}$$

Broadcast range and node degree: The node degree N_{p} is defined as the number of vehicular users falling in the broadcast range of a typical vehicular users. A vehicle can establish a communication link with a vehicle present in its broadcast range R_b. The node degree for a typical vehicular user is

$$\mathbb{P}\left[\widetilde{N}_{\mathrm{p}} = m\right] = \frac{1}{m!}\sum_{k=0}^{m}\binom{m}{k}\frac{\exp\left(-2\pi\lambda_{\boldsymbol{l}}R_b + g_{\mathrm{p},0}(R_b)\right)}{k!}\mathsf{B}\left(g_{\mathrm{p},1}(R_b),\ldots,g_{\mathrm{p},k}(R_b)\right)$$
$$\times\left(\lambda R_b\right)^k\exp\left(-\lambda R_b\right)$$

IV. Numerical Results

In this section, we first validates the obtained analytical PMFs with the simulation results.

Validation of approximation To validate the approximation with the exact simulation results, we plot the Bhattacharya's coefficient [23] of the approximations with the exact simulation results. The BC coefficients for the two PMF is $p(\omega)$ and $q(\omega)$ is defined as

$$D_{\mathrm{BC}}(p,q) = \sum_{\omega\in\Omega}\sqrt{p(\omega)q(\omega)}.$$

Here, we would like to highlight that that BC lies between 0 to 1, and closer to 1 denotes the better approximation. From Fig 1 we observe that the BC for the load on the typical and tagged BS is closer to 1. Therefore the approximation closely follows the simulation. Further we observe that the Approximation-1 have smaller BC coefficient than the Approximation-2 and therefore is not the exact results as suggested in [9].

Validation CD, NND and mean, variance for typical and tagged load The Fig. 2 shows the CD and NND for the Ψ_{p}. The simulations obtained are matching with analytical results. The Fig. 3 depicts the mean and variance of load on the typical and tagged BS. For the typical case, we have plotted the mean and the variance of both the approximations and the simulations. The mean load of the both approximations are coinciding with the simulations, however the variance shows a tremendous deviation for approximation-1 for smaller values of λ_b. Therefore,

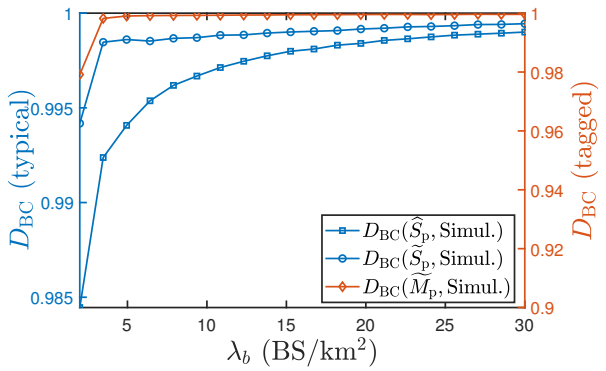

Fig. 1: The analytical expressions obtained using approximation closely follow simulation for the typical and tagged load distribution as the BC is close to 1.

the Approximation-2 is closer to the actual load distribution. For tagged case, we have only one expression. It can be observed that the mean coincides with the simulation results while the variance have deviations. For higher values of λ_b the variance start converging to the exact simulation results.

Validation of rate coverage and meta distribution The Fig. 4 (a) shows the rate coverage for two different values of threshold. We have plotted the active probability with the base station density λ_b. We see that the active probability closely matching with the simulation as it is an approximation. The active probability reduces with increase in the BS station density and therefore more and more BS will turn off and hence the power consumption reduces. The Fig. 4 (b) presents the meta distribution for the rate coverage. We have used the beta approximation to plot the meta distribution. The approximation closely follows the simulation.

Validation of SNR *distribution and node degree* The Fig. 5 (a) presents the SNR distribution upto 10 nearest vehicle from a typical BS. In the Fig.5 (b) and (c) we have shown the node degree for a typical vehicle. It is evident from the Fig. that node degree increases with the broadcast range of the vehicle.

V. Conclusion

In this paper, we have derived the PGF of the load on the typical and the tagged BS. Using the PGF, we have further derived corresponding mean and variance. We have presented the two approximations and compared the exact simulation results. We have shown that the Approximation-1 which is claimed in the literature to be the exact expression for the load on

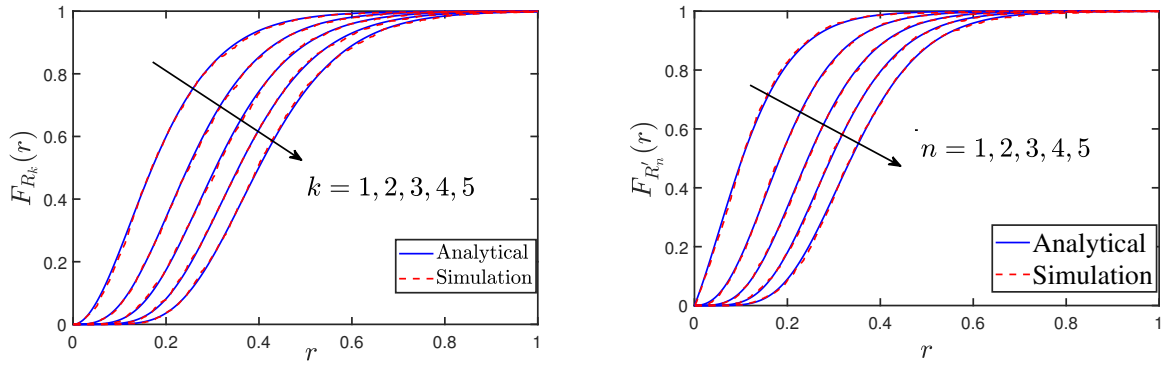

Fig. 2: The diagram showing the kth CD and NND for PLP-PPP. The parameters are $\lambda = 2$ vehicle/km, $\lambda_l = 5/\pi$ km and $\lambda_b = 1$ BS/km^2.

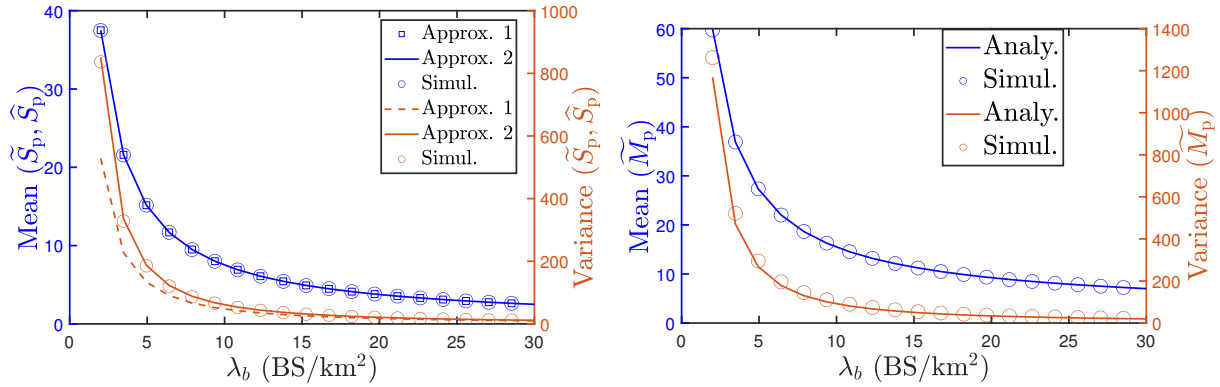

Fig. 3: The plot showing the mean and the variance for the load on the typical and the cell. The parameter are $\lambda_l = 5/\pi$ km^{-1}, $\lambda = 15$ vehicle/km. The Approx. 2 is closer to the simulations as compare to Approx. 1.

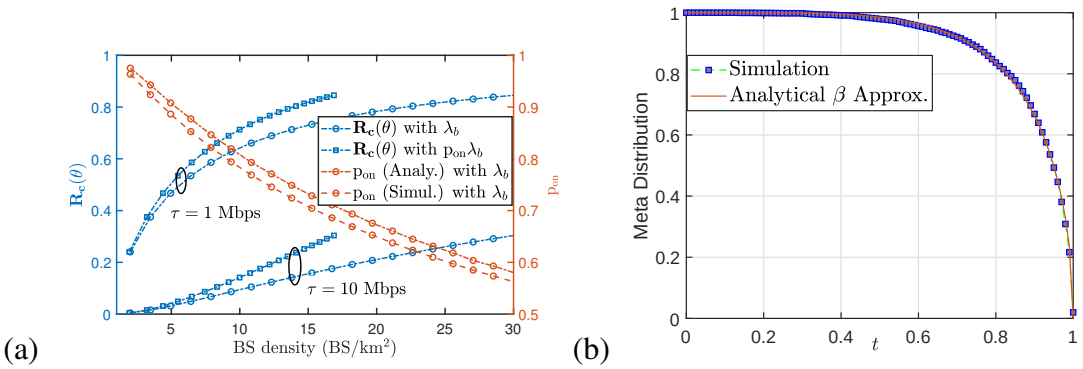

Fig. 4: Rate coverage for two different values of threshold. The values of $\alpha = 3.5$ and $B = 20$ MHz. The second Fig. presents the meta distribution for the PLP-PPP process. The parameters are $\mu_l = 5$, $\lambda = 2$ vehicles/km, $\lambda_b = 1/km^2$ and threshold rate $\tau = 0.1$ Mb.

the typical cell is actually another approximation. Further approximating the Voronoi with a circle provides the load distribution closer to the simulation. Using the load distribution, we

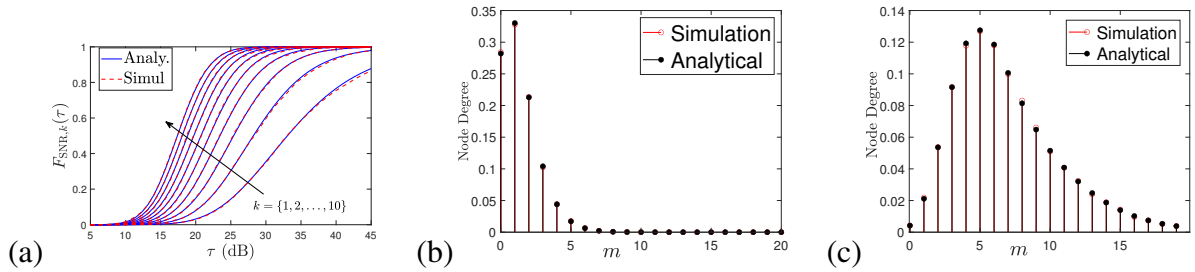

Fig. 5: Plot (a) showing the SNR distribution for 10 nearest vehicle from a typical BS. The plot (b) and (c) presents the node degree for the broadcast range $R_B = 10, 50$ m. Increasing the broadcast range increase the node degree of a typical vehicle.

have derived the rate coverage and meta distribution for the rate coverage. Using the method adopted in Approx.-2, we have derived the CDFs of kth CD and NND for PLP-PPP. We have shown two diffrent applications of distance distribution by deriving the SNR distribution from a BS to a typical vehicle and deriving the node degree.

APPENDIX

A. *Proof of Proposition-1*

We have considered an irregular convex n-gon with perimeter Z as shown in the Fig. 6. Using the triangular inequality we can obtain the following inequalities

$$|\mathrm{PP}_1| + |\mathrm{P}_1\mathrm{P}_2| \geq |\mathrm{PP}_2|,\ |\mathrm{PP}_2| + |\mathrm{P}_2\mathrm{P}_3| \geq |\mathrm{PP}_3|\ |\mathrm{PP}_3| + |\mathrm{P}_3\mathrm{Q}| \geq \mathrm{PQ} \tag{39}$$

From the above, it can be concluded that

$$|\mathrm{PP}_1| + |\mathrm{P}_1\mathrm{P}_2| + \mathrm{P}_2\mathrm{P}_3 + \mathrm{P}_3\mathrm{Q} \geq \mathrm{PQ}. \tag{40}$$

Similarly, we can proof that

$$|\mathrm{QP}_4| + |\mathrm{P}_4\mathrm{P}_5| + \ldots + |\mathrm{P}_{n-1}\mathrm{P}_n| + |\mathrm{P}_n\mathrm{P}| \geq |\mathrm{PQ}|. \tag{41}$$

Taking the summation of (40) and (41), we get the following

$$2|\mathrm{PQ}| \leq |\mathrm{P}_1\mathrm{P}_2| + |\mathrm{P}_2\mathrm{P}_3| + \ldots + |\mathrm{P}_{n-1}\mathrm{P}_n|,\ \Longrightarrow\ 2|\mathrm{PQ}| \leq Z, \tag{42}$$

solving the further completes the proof of Proposition-1.

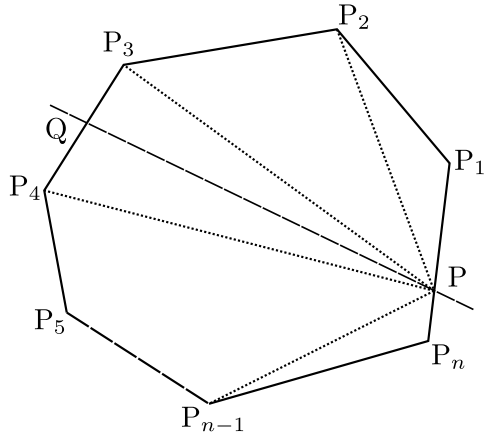

Fig. 6: The irregular convex n-gon with perimeter Z.

B. Proof of Proposition-2

To proof the dependency between the length of the chords we pic two chords in which we know the length of one chord. Further we show that the length of other chord is upper bounded by the length of given chord and a constant ϵ. Let the length of the given chord and unknown chords are C_1 and C_2 respectively. Using the technique presented in the proof of Proposition-1 we can proof the following inequality

$$C_2 \leq C_1 + \epsilon \, : \epsilon \in [0, Z/2] \tag{43}$$

The inequity 43, proves the dependency between the length distribution of two chords. Further, the length of a typical chord in a Voronoi with given perimeter is upper bounded by the half of the perimeter. Hence we truncate the distribution of $f_C(c)$ between 0 to $Z/2$ [**?**].

C. Proof of Lemma-1

The number of points falling in the typical cell (typical Voronoi) is

$$\widehat{S}_{\mathrm{p}} = \sum_{\boldsymbol{l}_k \in \Phi} \psi_{\boldsymbol{l}_k} \left(V_{\mathrm{t}} \right).$$

Let n be the number of chords intersecting a typical Voronoi cell. The PGF expression is

$$\mathcal{P}_{\widehat{S}_{\mathrm{p}}|N}(s) = \mathbb{E}_{\Psi_{\mathrm{p}}} \left[s^{\widehat{S}_{\mathrm{p}}} \Big| N = n \right] = \mathbb{E}_{\Psi_{\mathrm{p}}} \left[\prod_{k=1}^{n} s^{\psi_{\boldsymbol{l}_k}(V_{\mathrm{t}})} \Big| N = n \right] = \left[\int_0^{z/2} e^{h(s,c)} f_C^{'}(c) \mathrm{d}c \right]^n,$$

where $h(s,c) = \lambda c(s-1)$. As the number of chords intersecting a typical Voronoi n is Poisson random variable with mean $\lambda_{\boldsymbol{l}} Z$, where Z denotes the perimeter of typical Voronoi. Hence conditioned on $Z = z$, first we decondition over n to get the PGF as

$$\mathcal{P}_{\widehat{S}_{\mathrm{p}}|Z=z}(s) = \sum_{n=0}^{\infty} \frac{e^{-\lambda_{\boldsymbol{l}} z} (\lambda_{\boldsymbol{l}} z)^n}{n!} \mathcal{P}_{\widehat{S}_{\mathrm{p}}|N}(s) = e^{-\lambda_{\boldsymbol{l}} z \left(1 - \int_0^{z2} e^{h(s,c)} f_C(c) \mathrm{d}c\right)}. \tag{44}$$

Deconditioning with the distribution of Z, we get the PGF. From the PGF of $\widehat{S}_{\mathrm{p}}$, we get the PMF of $\widehat{S}_{\mathrm{p}}$ as

$$\mathbb{P}\left[\widehat{S}_{\mathrm{p}}=k\right]=\left[\mathcal{P}^{(k)}_{\widehat{S}_{\mathrm{p}}}(s)/k!\right]_{s=0}=(1/k!)\int_{z=0}^{\infty}\mathcal{P}^{(k)}_{\widehat{S}_{\mathrm{p}}|Z}(s)f_{Z=z}(z)\mathrm{d}z. \tag{45}$$

The conditional PGF $\mathcal{P}_{\widehat{S}_{\mathrm{p}}|Z}(s)$ is in form of $\exp(\cdot)$. The kth derivative of conditional PGF can be determined using (4). After obtaining the kth derivative using (45) we get the PMF of S_{p}.

D. Proof of Theorem 2

Let $\psi_{\boldsymbol{l}_k}(\mathbf{b}_2(\mathrm{o},r_{\mathrm{t}}))$ denotes number of vehicles on kth road of Φ falling inside ball $\mathbf{b}_2(\mathrm{o},r_{\mathrm{t}})$.

$$\widetilde{S}_{\mathrm{p}}=\sum_{\boldsymbol{l}_k\in\Phi}\psi_{\boldsymbol{l}_k}\left(\mathbf{b}_2(\mathrm{o},r_{\mathrm{t}})\right).$$

A road $\boldsymbol{l}$ which is ρ distance away from the origin o have the length $2\sqrt{r_{\mathrm{t}}^2-\rho^2}$. The average number of point falling inside $\mathbf{b}_2(\mathrm{o},r_{\mathrm{t}})$ located on $\boldsymbol{l}$ is $2\lambda\sqrt{r_{\mathrm{t}}^2-\rho^2}$. Hence conditioned on $R_{\mathrm{t}}=r_{\mathrm{t}}$ and ρ the PGF of number of points falling on the line inside $\mathbf{b}_2(\mathrm{o},r_{\mathrm{t}})$ is

$$\mathcal{P}_{\psi_{\boldsymbol{l}}(\mathbf{b}_2(\mathrm{o},r_{\mathrm{t}}))|\rho,R_{\mathrm{t}}}\left(s,\sqrt{r_{\mathrm{t}}^2-\rho^2}\right)=e^{h\left(s,\sqrt{r_{\mathrm{t}}^2-\rho^2}\right)},$$

where $h\left(s,\sqrt{r_{\mathrm{t}}^2-\rho^2}\right)=2\lambda\sqrt{r_{\mathrm{t}}^2-\rho^2}(s-1)$. Note that ρ is a uniform random variable in the range $[-r_{\mathrm{t}},\,r_{\mathrm{t}}]$. Hence, deconditioning over ρ the PGF expression reduces to

$$\mathcal{P}_{\widetilde{S}_{\mathrm{p}}|R_{\mathrm{t}}}(s,r_{\mathrm{t}})=\frac{1}{2r_{\mathrm{t}}}\int_{-r_{\mathrm{t}}}^{r_{\mathrm{t}}}e^{\left(h\left(s,\sqrt{r_{\mathrm{t}}^2-\rho^2}\right)\right)}\mathrm{d}\rho\overset{(a)}{=}\int_{t=0}^{r_{\mathrm{t}}}\frac{e^{h(s,t)}t\mathrm{d}t}{\sqrt{t^2-\rho^2}},$$

replacing $\sqrt{r_{\mathrm{t}}^2-\rho^2}=t$, we get the step (a). Let there be n such lines hence the joint PGF is the product of individual PGFs of n line which is equal to

$$\mathcal{P}_{\widetilde{S}_{\mathrm{p}}|N,R_{\mathrm{t}}}(s,r_{\mathrm{t}})=\left(\int_{t=0}^{r_{\mathrm{t}}}\frac{e^{h(s,t)}t\mathrm{d}t}{\sqrt{t^2-\rho^2}}\right)^n,$$

here n is a Poisson RV with mean $\lambda_{\boldsymbol{l}}2\pi r_{\mathrm{t}}$. From the law of total probability deconditioning over n we get the PGF conditioned on $R_{\mathrm{t}}=r_{\mathrm{t}}$. Finally deconditioning over R_{t}, we get the PGF of $\widetilde{S}_{\mathrm{p}}$. Thee PGF $\mathcal{P}_{S'_{\mathrm{p}}}(s)$ can be written as

$$\mathcal{P}_{\widetilde{S}_{\mathrm{p}}}(s)=\int_0^{\infty}\exp\left(g_{\mathrm{p}}\left(s,r_{\mathrm{t}}\right)\right)f_{R_{\mathrm{t}}}(r_{\mathrm{t}})\mathrm{d}r_{\mathrm{t}},$$

where $g_{\mathrm{p}}(s,r_{\mathrm{t}})$ is

$$g_{\mathrm{p}}(s,r_{\mathrm{t}})=2\pi\lambda_{\boldsymbol{l}}\left(\int_0^{r_{\mathrm{t}}}\frac{\exp\left(2\lambda(s-1)t\right)t\mathrm{d}t}{\sqrt{r_{\mathrm{t}}^2-t^2}}-r_{\mathrm{t}}\right) \tag{46}$$

Hence, the kth derivative $\mathcal{P}^{(k)}_{\widetilde{S}_\mathrm{p}}(s, r_\mathrm{t})$ with respect to s is given by

$$\mathcal{P}^{(k)}_{\widetilde{S}_\mathrm{p}}(s) \overset{(a)}{=} \int_0^\infty \exp\left(g_\mathrm{p}(s, r_\mathrm{t})\right) \mathsf{B}\left(g^{(1)}_\mathrm{p}(s, r_\mathrm{t}), ...g^{(k)}_\mathrm{p}(s, r_\mathrm{t})\right) f_{R_\mathrm{t}}(r_\mathrm{t}) \mathrm{d}r_\mathrm{t}, \tag{47}$$

the step (a) is obtained using the Faà di Bruno's formula [13]. The $g^{(k)}_\mathrm{p}(s, r_\mathrm{t})$ can be written as

$$= 2\pi\lambda_{\boldsymbol{l}} \int_0^{r_\mathrm{t}} (2\lambda t)^k \frac{\exp\left((s-1)2\lambda t\right)}{\sqrt{r_\mathrm{t}^2 - t^2}} t \mathrm{d}t. \tag{48}$$

From (47), (48) and replacing $s = 0$, we get the PMF of $\widetilde{S}_\mathrm{p}$.

E. Proof of Corollary 2.1

To derive the variance of $\widetilde{S}_\mathrm{p}$, we need the second derivative of the PGF that is given as

$$\left[\mathcal{P}^2_{\widetilde{S}_\mathrm{p}}(s)\right]_{s=1} = \int_0^\infty \left[\left(2\pi\lambda_{\boldsymbol{l}}(2\lambda) \int_0^{r_\mathrm{t}} \frac{t^2}{\sqrt{r_\mathrm{t}^2 - t^2}} \mathrm{d}t\right)^2 + 2\pi\lambda_{\boldsymbol{l}}(2\lambda)^2 \int_0^{r_\mathrm{t}} \frac{t^3}{\sqrt{r_\mathrm{t}^2 - t^2}} \mathrm{d}t\right] f_{R_\mathrm{t}}(r_\mathrm{t}) \mathrm{d}r_\mathrm{t}$$

$$= \int_0^\infty \left[\left(4\pi\lambda_{\boldsymbol{l}}\lambda \frac{\pi}{4} r_\mathrm{t}^2\right)^2 + 8\pi\lambda_{\boldsymbol{l}}\lambda^2 \frac{2}{3} r_\mathrm{t}^3\right] f_{R_\mathrm{t}}(r_\mathrm{t}) \mathrm{d}r_\mathrm{t} = (\pi\lambda_\mathrm{p})^2 \mathbb{E}[r_\mathrm{t}^4] + \frac{16}{3}\lambda\lambda_\mathrm{p}\mathbb{E}[r_\mathrm{t}^3].$$

Using the (1) and the second derivative, we derive the variance of $\widetilde{S}_\mathrm{p}$. To derive the mean and the variance using the Approximation-1, the first derivative of the PGF is

$$\left[\mathcal{P}^{(1)}_{\hat{S}_\mathrm{p}}(s)\right]_{s=1} = \int_{z=0}^\infty \lambda_{\boldsymbol{l}} z \int_0^\infty \lambda c f_C(c) \mathrm{d}c f_Z(z) \mathrm{d}z$$

$$= \lambda_{\boldsymbol{l}}\lambda \int_0^\infty c f_C(c) \mathrm{d}c \int_{z=0}^\infty z f_Z(z) \mathrm{d}z,$$

solving further we get the mean of $\widehat{S}_\mathrm{p}$. To get the variance of $\widehat{S}_\mathrm{p}$, we need the second derivative of $\mathcal{P}_{\widehat{S}_\mathrm{p}}(s)$ which is given as

$$\mathcal{P}^{(2)}_{\widehat{S}_\mathrm{p}}(s) = \left(\lambda_{\boldsymbol{l}}\lambda\mathbb{E}[C]\right)^2 \mathbb{E}[Z^2] + \lambda_{\boldsymbol{l}}\lambda^2 \mathbb{E}[Z]\mathbb{E}[C^2],$$

using (1), we get the variance of $\widehat{S}_\mathrm{p}$.

F. Proof of Theorem 3

The $\widetilde{M}_\mathrm{p}$ is sum of two independent RV, the first is the number of points falling on chord of length c_o and the second is number of vehicles falling inside ball of radius r_o.

$$\widetilde{M}_\mathrm{p} = \psi_{\boldsymbol{l}_\mathrm{o}}\left(\mathbf{b}_1\left(\mathrm{o}, c_\mathrm{o}/2\right)\right) + \Psi_\mathrm{p}(\mathbf{b}_2(\mathrm{o}, r_\mathrm{o})), \tag{49}$$

where $\psi_{\boldsymbol{l}_\mathrm{o}}\left(\mathbf{b}_1\left(\mathrm{o}, c_\mathrm{o}/2\right)\right)$ denotes the number of points on tagged chord of length c_o with PGF $\exp\left(\lambda c_\mathrm{o}(s-1)\right)$ and $\Psi_\mathrm{p}(\mathbf{b}_2(\mathrm{o}, r_\mathrm{o}))$ denotes the number of points of Ψ_p falling inside a ball of radius r_o and the area is equal to the area of Voronoi cell $V_{\mathrm{t}_\mathrm{o}}$. The PGF of $\Psi_\mathrm{p}(\mathbf{b}_2(\mathrm{o}, r_\mathrm{o}))$ can determined using the Theorem 2. Multiplying the two PGFs we get the PGF of $\widetilde{M}_\mathrm{p}$.

G. Proof of Theorem 5

The coverage probability conditioned on the nearest BS distance R is

$$P_{\mathrm{r}}(\tau) = \mathbb{E}\left[\mathbb{P}\left(\text{SIR} > \tau\right)|\Phi_b\right] = \mathbb{E}\left[\mathbb{P}\left(\frac{h_0 r^{-\alpha}}{I} > \tau\right)\right]$$
$$= \mathbb{E}\left[\mathbb{P}\left(h_0 > \tau I r^{\alpha}\right)\right] = \left[\mathbb{E}\left[\exp\left(-\tau I r^{\alpha}\right)|\Phi_b\right]\right] \overset{(a)}{=} \left[\frac{1}{1+\tau r^{\alpha}||\mathbf{y}||^{-\alpha}}\right],$$

here (a) is obtained using the LF of interference [24]. Hence the qth moment of $P_{\mathrm{r}}(\tau)$ is

$$\mathsf{M}_q(\tau) = \mathbb{E}_{\Phi_b}\left[\prod_{\mathbf{y}\in\Phi_b} \frac{1}{(1+\tau r^{\alpha}||\mathbf{y}||^{-\alpha})^q}\Big| R\right],$$

using the PGFL of PPP and deconditioning over R, we get the q-th moment of the coverage probability.

$$= 2\pi\lambda_b \int_{r=0}^{\infty} \exp\left(-2\pi \mathrm{p}_{\mathrm{on}}\lambda_b \int_r^{\infty}\left(1 - \frac{1}{(1+\tau r^{\alpha} y^{-\alpha})^q}\right) y\mathrm{d}y\right) e^{-\lambda_b \pi r^2} r\mathrm{d}r,$$

which further simplified by replacing $r/y = z$ and $\lambda_b \pi r^2 = u$ which completes the proof of Theorem 5. Further the q-th moment of the rate coverage is

$$\mathsf{S}_q(\theta(\tau)) = \mathbb{E}\left[\left(\mathbb{P}\left((\mathcal{R} > \tau)\left|\Phi_b, \widetilde{M}_{\mathrm{p}}\right.\right)\right)^q\right]$$
$$= \mathbb{E}\left[\left(\mathbb{P}\left(\frac{B}{\widetilde{M}_{\mathrm{p}}+1}\log_2\left(1+\text{SIR}\right) > \tau\right)\Big|\, \Phi_b, \widetilde{M}_{\mathrm{p}}\right)^q\right]$$
$$= \mathbb{E}\left[\left(\mathbb{P}\left(\left(\text{SIR} > 2^{\frac{(\widetilde{M}_{\mathrm{p}}+1)\tau}{B}} - 1\right)\Big|\Phi_b, \widetilde{M}_{\mathrm{p}}\right)\right)^q\right]$$
$$= \left[\mathbb{P}\left(\mathsf{M}_q\left(\theta(\tau)\right)\Big|\widetilde{M}_{\mathrm{p}}\right)\right],$$

where $\theta(\tau) = 2^{\frac{(\widetilde{M}_{\mathrm{p}}+1)\tau}{B}} - 1$. deconditioning over $\widetilde{M}_{\mathrm{p}}$, we get the qth moment of rate coverage probability.

H. Proof of Theorem 6

From the definition of meta distribution

$$\overline{F}_{P_{\mathrm{r}}(\tau)}(x) = \mathbb{P}(P_{\mathrm{r}}(\tau) > x)$$
$$= \frac{1}{2} + \frac{1}{\pi}\int_0^{\infty} \frac{\mathsf{Im}\left[e^{-it\ln(x)}\mathsf{S}_{it}(\theta(\tau))\right]}{t}\mathrm{d}t$$
$$= \frac{1}{2} + \frac{1}{\pi}\sum_{m=0}^{\infty}\mathbb{P}(\widetilde{M}_{\mathrm{p}} = m)\int_{t=0}^{\infty}\frac{\mathrm{Im}\left[e^{-it\ln(x)}\mathsf{M}_{it}\left(\theta(\tau)\right)\right]}{t}\mathrm{d}t$$

We can further simplify the above expression to extract the imaginary part of the above equation.

$$\mathsf{M}_{it}(\theta(\tau)) = \int_{u=0}^{\infty}\exp\left(-2\mathrm{p}_{\mathrm{on}}u\int_0^1\left(1 - \frac{1}{\left(1+\theta(\tau)z^{\alpha}\right)^{it}}\right)\frac{\mathrm{d}z}{z^3}\right)e^{-u}\mathrm{d}u$$

we can write

$$(1+\theta(\tau)z^{\alpha})^{-it} = e^{-it\ln(1+\theta(\tau)z^{\alpha})} = \cos\left(t\ln\left(1+\theta(\tau)z^{\alpha}\right)\right) - i\sin\left(t\ln\left(1+\theta(\tau)z^{\alpha}\right)\right)$$
$$= f_r(t,\theta(\tau),z) - if_i(t,\theta(\tau),z);$$

replacing the above and simplifying further we get

$$\mathsf{M}_{it}(\theta(\tau)) = \int_{u=0}^{\infty}\exp\left(-2\mathrm{p}_{\mathrm{on}}u\int_{z=0}^{1}\left(1-f_r(t,\theta(\tau),z)+if_i(t,\theta(\tau),z)\right)\frac{\mathrm{d}z}{z^3}\right)e^{-u}\mathrm{d}u$$
$$= \int_{u=0}^{\infty}\exp\left(-u2\mathrm{p}_{\mathrm{on}}\int_{z=0}^{1}\left(1-f_r(t,\theta(\tau),z)\right)\frac{\mathrm{d}z}{z^3}\right)\exp\left(-iu2\mathrm{p}_{\mathrm{on}}\int_{z=0}^{1}f_i(t,\theta(\tau),z)\frac{\mathrm{d}z}{z^3}\right)e^{-u}\mathrm{d}u$$

Let $f_{1,i}(t,\theta(\tau)) = 2\mathrm{p}_{\mathrm{on}}\int_{z=0}^{1}\left(1-f_i(t,\theta(\tau),z)\right)\frac{\mathrm{d}z}{z^3}$ and $f_{1,r}(t,\theta(\tau)) = 2\mathrm{p}_{\mathrm{on}}\int_{z=0}^{1}\left(1-f_r(t,\theta(\tau),z)\right)\frac{\mathrm{d}z}{z^3}$.

$$\mathsf{Im}\left[e^{-it\ln(x)}\mathsf{M}_{it}\left(\theta(\tau)\right)\right] = \mathsf{Im}\left(\int_{u=0}^{\infty}\exp\left(-uf_{1,r}(t,\theta(\tau))\right)\exp\left(-i\left(t\ln(x)+uf_{1,i}(t,\theta(\tau))\right)\right)\right)e^{-u}\mathrm{d}u$$
$$= -\int_{u=0}^{\infty}\exp\left(-uf_{1,r}(t,\theta(\tau))\right)\sin\left(t\ln(x)+uf_{1,i}(t,\theta(\tau))\right)e^{-u}\mathrm{d}u$$

Therefore the meta distribution $\overline{F}_{P_{\mathrm{r}}(\tau)}(x)$ reduces to

$$= \frac{1}{2} - \frac{1}{\pi}\sum_{m=0}^{\infty}\mathbb{P}(\widetilde{M}_{\mathrm{p}}=m)\int_{t=0}^{\infty}\int_{u=0}^{\infty}\exp\left(-uf_{1,r}(t,\theta(\tau))\right)\sin\left(t\ln(x)+uf_{1,i}(t,\theta(\tau))\right)e^{-u}\mathrm{d}u\frac{\mathrm{d}t}{t}.$$

Substituting the above and simplifying further, we get

$$= \frac{1}{2} - \frac{1}{\pi}\sum_{m=0}^{\infty}\mathbb{P}(\widetilde{M}_{\mathrm{p}}=m)\int_{t=0}^{\infty}\int_{u=0}^{\infty}\exp\left(-u\left(1+f_{1,r}(t,\theta(\tau))\right)\right)\sin\left(t\ln(x)+uf_{1,i}(t,\theta(\tau))\right)\mathrm{d}u\frac{\mathrm{d}t}{t},$$
$$\overset{(a)}{=} \frac{1}{2} - \frac{1}{\pi}\sum_{m=0}^{\infty}\mathbb{P}(\widetilde{M}_{\mathrm{p}}=m)\int_{t=0}^{\infty}\frac{f_{1,i}(t,\theta(\tau))\cos\left(t\ln(x)\right)+\left(\left(f_{1,r}(t,\theta(\tau)+1\right)\sin\left(t\ln(x)\right)\right)}{\left(f_{1,r}(t,\theta(\tau))+1\right)^2+\left(f_{1,i}(t,\theta(\tau))\right)^2}\frac{\mathrm{d}t}{t},$$

here step (a) is obtained by apply $\sin\left(t\ln(x)+uf_{1,i}(t,\theta(\tau))\right) = \sin(t\ln(x))\cos\left(uf_{1,i}(t,\theta(\tau))\right)+\cos(t\ln(x))\sin\left(uf_{1,i}(t,\theta(\tau))\right)$ and than using the following integral identity

$$\int_0^{\infty}e^{-ax}\sin(bx) = \frac{b}{a^2+b^2},\ \int_0^{\infty}e^{-ax}\cos(bx) = \frac{a}{a^2+b^2}.$$

Solving further from step (a), we get the meta distribution for the rate coverage.

REFERENCES

[1] M. Haenggi, *Stochastic geometry for wireless networks*. Cambridge University Press, 2012.

[2] S. N. Chiu, D. Stoyan, W. S. Kendall, and J. Mecke, *Stochastic geometry and its applications*. John Wiley & Sons, 2013.

[3] H. S. Dhillon and V. V. Chetlur, *Poisson Line Cox Process: Foundations and Applications to Vehicular Networks*. Morgan & Claypool Publishers, 2020.

[4] C.-S. Choi and F. Baccelli, "Poisson Cox point processes for vehicular networks," *IEEE Trans. Veh. Technol*, vol. 67, no. 10, pp. 10 160–10 165, 2018.

[5] V. V. Chetlur and H. S. Dhillon, "Coverage and rate analysis of downlink cellular vehicle-to-everything (C-V2X) communication," *IEEE Trans. Wireless Commun.*, vol. 19, no. 3, pp. 1738–1753, 2019.

[6] S. Guha, "Cellular-assisted vehicular communications: A stochastic geometric approach," M.S. thesis, Virginia Tech, 2016.

[7] C.-S. Choi and F. Baccelli, "An analytical framework for coverage in cellular networks leveraging vehicles," *IEEE Trans. on Commun.*, vol. 66, no. 10, pp. 4950–4964, 2018.

[8] M. N. Sial, Y. Deng, J. Ahmed, A. Nallanathan, and M. Dohler, "Stochastic geometry modeling of cellular V2X communication over shared channels," *IEEE Trans. Veh. Technol*, vol. 68, no. 12, pp. 11 873–11 887, 2019.

[9] V. V. Chetlur and H. S. Dhillon, "On the load distribution of vehicular users modeled by a Poisson line Cox process," *IEEE Wireless Commun. Lett.*, vol. 9, no. 12, pp. 2121–2125, 2020.

[10] ——, "Coverage analysis of a vehicular network modeled as Cox process driven by Poisson line process," *IEEE Trans. Wireless Commun.*, vol. 17, no. 7, pp. 4401–4416, 2018.

[11] V. V. Chetlur, S. Guha, and H. S. Dhillon, "Characterization of V2V coverage in a network of roads modeled as Poisson line process," in *Proc. IEEE ICC*, 2018, pp. 1–6.

[12] M. Afshang, C. Saha, and H. S. Dhillon, "Nearest-neighbor and contact distance distributions for Thomas cluster process," *IEEE Wireless Commun. Lett.*, vol. 6, no. 1, pp. 130–133, 2016.

[13] W. P. Johnson, "The curious history of Faà di Bruno's formula," *The American Mathematical Monthly*, vol. 109, no. 3, pp. 217–234, 2002.

[14] M. Tanemura, "Statistical distributions of Poisson Voronoi cells in two and three dimensions," *FORMA-TOKYO-*, vol. 18, no. 4, pp. 221–247, 2003.

[15] L. Muche and D. Stoyan, "Contact and chord length distributions of the Poisson Voronoi tessellation," *J. Appl. Probab.*, vol. 29, no. 2, pp. 467–471, 1992.

[16] A. K. Gupta, X. Zhang, and J. G. Andrews, "Potential throughput in 3D ultradense cellular networks," in *Proc. Asilomar Conference on Signals, Systems and Computers*, 2015, pp. 1026–1030.

[17] M. Haenggi, "The meta distribution of the SIR in Poisson bipolar and cellular networks," *IEEE Trans. Wireless Commun.*, vol. 15, no. 4, pp. 2577–2589, 2015.

[18] J. Gil-Pelaez, "Note on the inversion theorem," *Biometrika*, vol. 38, no. 3-4, pp. 481–482, 1951.

[19] N. Deng and M. Haenggi, "A Fine-Grained Analysis of Millimeter-Wave Device-to-Device Networks," *IEEE Trans. Commun.*, vol. 65, no. 11, pp. 4940–4954, 2017.

[20] K. Koufos, H. S. Dhillon, M. Dianati, and C. P. Dettmann, "On the k nearest-neighbor path distance from the typical intersection in the manhattan poisson line cox process," *IEEE Trans. Mobile Comput*, 2021.

[21] K. Pandey and A. K. Gupta, "kth Distance distributions of n-dimensional Matérn cluster process," *IEEE Commun. Lett.*, vol. 25, no. 3, pp. 769–773, 2021.

[22] J. B. Andersen, T. S. Rappaport, and S. Yoshida, "Propagation measurements and models for wireless communications channels," *IEEE Communications magazine*, vol. 33, no. 1, pp. 42–49, 1995.

[23] A. Bhattacharyya, "On a measure of divergence between two multinomial populations," *Sankhyā: the Indian journal of statistics*, pp. 401–406, 1946.

[24] J. G. Andrews, A. Gupta, and H. S. Dhillon, "A primer on cellular network analysis using stochastic geometry," *arXiv 1604.03183*, 2016.